



Chaos game representation of the D_{st} index and prediction of geomagnetic storm events

Z.G. Yu^{a,d}, V.V. Anh^{a,c,*}, J.A. Wanliss^b, S.M. Watson^c

^a Program in Statistics and Operations Research, Queensland University of Technology, GPO Box 2434, Brisbane Q4001, Que., Australia

^b Embry-Riddle Aeronautical University, 600 S. Clyde Morris Blvd. Daytona Beach, Florida, FL 32114, USA

^c Florida Space Institute, University of Central Florida, Orlando, FL 32816-2370, USA

^d School of Mathematics and Computational Science, Xiangtan University, Hunan 411105, China

Accepted 21 December 2005

Abstract

This paper proposes a two-dimensional chaos game representation (CGR) for the D_{st} index. The CGR provides an effective method to characterize the multifractality of the D_{st} time series. The probability measure of this representation is then modeled as a recurrent iterated function system in fractal theory, which leads to an algorithm for prediction of a storm event. We present an analysis and modeling of the D_{st} time series over the period 1963–2003. The numerical results obtained indicate that the method is useful in predicting storm events one day ahead.

© 2006 Elsevier Ltd. All rights reserved.

1. Introduction

A measure of the strength of a magnetic storm is the D_{st} index, which reflects the variations in the intensity of the symmetric part of the ring current at altitudes ranging from about 3–8 earth radii [11,19]. The D_{st} is calculated as an hourly index from the horizontal magnetic field component at four observatories, namely, Hermanus (33.3° south, 80.3° in magnetic dipole latitude and longitude), Kakioka (26.0° north, 206.0°), Honolulu (21.0° north, 266.4°), and San Juan (29.9° north, 3.2°). These four observatories were chosen because they are close to the magnetic equator and thus are not strongly influenced by auroral current systems.

In the recent literature, fractal and multifractal approaches have been quite successful in extracting salient features of physical processes responsible for the near-Earth magnetospheric phenomena [24]. Heavy-tailed Lévy-type behavior, particularly that of stable distributions, has also been observed in the interplanetary magnetic field and the magnetosphere [8–10,22,23,25]. It has been found that D_{st} exhibits a power-law spectrum with the Hurst index varying over different stretches of the time series [28,29]. This behavior indicates that D_{st} is a multifractal process which has an important example—multifractional Brownian motion [4]. A method to describe the multiple scaling of the measure representation of the D_{st} time series was provided in [30]. This measure is modeled as a recurrent iterated function

* Corresponding author. Address: Program in Statistics and Operations Research, School of Math, Queensland University of Technology, GPO Box 2434, Brisbane Q4001, Que., Australia. Tel.: +61 7 3864 2317; fax: +61 7 3864 2310.

E-mail address: v.anh@qut.edu.au (V.V. Anh).

system (RIFS, [7]), which is considered as a dynamical system. The attractor of this dynamical system is in fact the support of its invariant measure which models the measure representation of the D_{st} . The probability of a specific pattern of events can be obtained from the RIFS; hence the method provides a mechanism for prediction of storm patterns included in the attractor of the RIFS. This prediction method was detailed in [3] together with some numerical results evaluating its performance.

It is noted that the measure representation used in [3,30] is a representation of the probabilities of the patterns of events computed from a given time series. Hence the resulting RIFS yields the probability of a pattern of future events. In this paper, we look at the multiple scaling of D_{st} from a different angle, namely from that of the probability measure of its chaos game representation (CGR) defined below. CGR has been used to represent DNA sequences [21], protein structures [17], linked protein sequences from genomes [33], the two-slit experiment of quantum mechanics [12–15] for example. The CGR records the relative position of an event rather than the probability of a pattern of events. The resulting probability measure also has the characteristic of a multifractal measure, and will be modeled via a recurrent iterated function system, hence again can be used for prediction purposes. It should be emphasized that the RIFS of a measure representation models a pattern (of 12 events), for example, as described in [3], hence its prediction of a future event relies on the history of past events (for example, the occurrence of the previous 11 events). On the other hand, the RIFS of the CGR gives the weighting of a single event, and its prediction is based solely on the position of the previous event in the CGR. It is therefore expected that prediction based on the CGR method is more difficult than that based on the measure representation method; however, the CGR method provides needed information on a future event if it works, rather than conditional information as in the measure representation method.

The next section will outline the concepts of chaos game representation, multifractal measures and RIFS. Section 3 develops RIFS models for the probability measure of the CGR of the daily D_{st} time series. The invariant measure of the RIFS is then obtained, which is shown to trace out closely the probability measure of the given time series. This model is then used to generate future storm events via the chaos game algorithm. The performance of this prediction method will be evaluated through two accuracy indicators. Some concluding comments on the approach will be provided in Section 4.

2. Iterated function systems for multifractal measures

2.1. Chaos game representation

This paper will develop models for the CGR of storm events. The proposed method examines the multiple scaling of a process via the probability measure of its CGR. We first describe the derivation of a symbolic sequence from a time series. We assume that this time series can be classified into a number of different categories. For example, the D_{st} index is clustered into four categories: $D_{st} \leq -100$; $-100 < D_{st} \leq -50$; $-50 < D_{st} \leq -30$; $-30 < D_{st}$, which correspond to intense-, moderate-, small-storm and no-storm types respectively. We then define the map

$$f_1 = \begin{cases} 0, & \text{if } D_{st} > -30 \text{ nT}, \\ 1, & \text{if } -50 \text{ nT} < D_{st} \leq -30 \text{ nT}, \\ 2, & \text{if } -100 \text{ nT} < D_{st} \leq -50 \text{ nT}, \\ 3, & \text{if } D_{st} \leq -100 \text{ nT}. \end{cases}$$

Under f_1 , the given D_{st} time series is transformed into a symbolic sequence $\{s_i\}$, where s_i is a symbol of the alphabet $\{0, 1, 2, 3\}$.

We next define the chaos game representation for the sequence $\{s_i\}$ in the square $[0, 1] \times [0, 1]$, where the four vertices correspond to the four symbols 0, 1, 2, 3: The first point of the plot is located half way between the center of the square and the vertex corresponding to the first symbol of the sequence $\{s_i\}$; the i th point of the plot is then located half way between the $(i - 1)$ th point and the vertex corresponding to the i th symbol. We then call the obtained plot the *chaos game representation* of the given D_{st} time series. It is noted that the map f_1 is a one-to-one correspondence between the symbolic sequence $\{s_i\}$ and its CGR, and the sequence $\{s_i\}$ can be reconstructed uniquely from its CGR given a starting point.

As an example, we consider the D_{st} index (further detail on this index is provided in Section 3.1). In this example, we created a daily time series by taking the minimum value for each day of the original D_{st} series, which is available in hourly resolution from 1963 to the present time. The daily series is displayed for the period 1963–2003 as an illustration in Fig. 1. Its CGR is provided in Fig. 2. Self-similarity is apparent in the D_{st} series via its CGR.

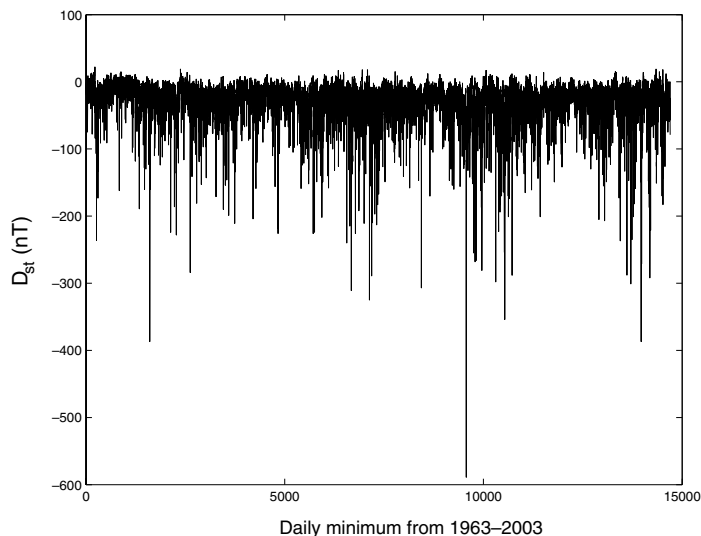


Fig. 1. The daily D_{st} time series from 1963–2003.

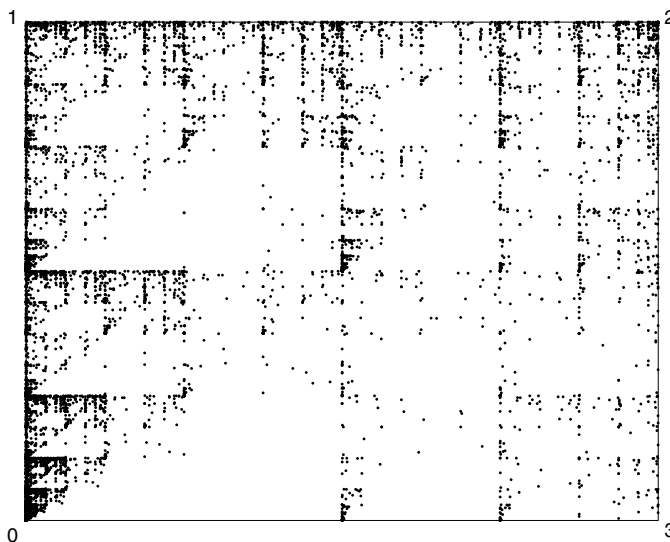


Fig. 2. The four-symbol CGR of daily D_{st} time series from 1963–2003.

Considering the set of points in a CGR of a time series, we can define a measure μ by $\mu(B) = \#(B)/N_1$, where $\#(B)$ is the number of points lying in a subset B of the CGR and N_1 is the length of the sequence. We can divide the square $[0, 1] \times [0, 1]$ into meshes of size 64×64 , 128×128 , 512×512 or 1024×1024 . This results in a measure, in fact a probability measure by its definition, for each mesh. The measure μ based on a 128×128 mesh of the CGR of Fig. 2 is given in Fig. 3 as an example.

2.2. Multifractal measures

Magnetic storms are apparently dynamic over many time scales. The D_{st} time series is highly intermittent. This behavior is characterized by the different values of the generalized dimension of its measure, which is then known as a multifractal measure.

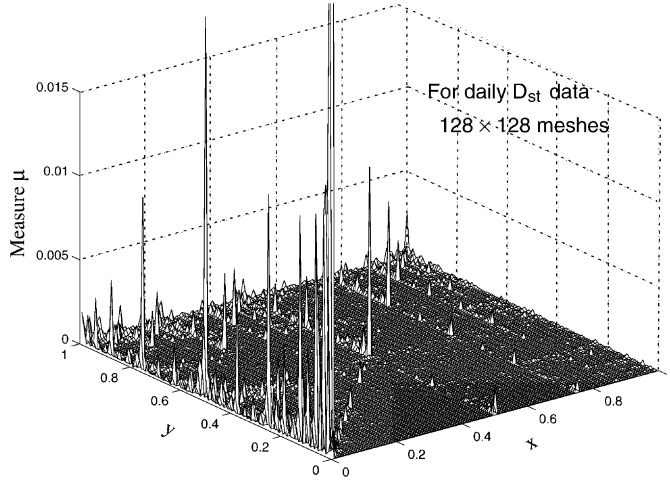


Fig. 3. The measure μ based on a 128×128 mesh of the CGR of Fig. 2.

We will be concerned with the two-dimensional case, that is, a measure μ with support $A \subset \mathbb{R}^2$ (commonly normalized to have mass $\mu(A) = 1$). The generalized dimension of a measure μ can be defined using the box-counting method [20] as

$$D_q = \lim_{\epsilon \rightarrow 0} \frac{\ln(\sum_i (M_i/M_0)^q)}{\ln(\epsilon)} \frac{1}{q-1}, \quad q \in \mathbb{R}, \quad (2.1)$$

where ϵ is the ratio of the grid size to the linear size of the support A , M_i the number of points fall in the i th grid cell, M_0 the total number of points in A .

For feasible computation of the generalized dimension on real data. Tél et al. [26] introduced a *sandbox* method which is defined by

$$D_q = \lim_{R \rightarrow 0} D_q(R/L) = \lim_{R \rightarrow 0} \frac{\ln(\langle [M(R)/M_0]^{q-1} \rangle)}{\ln(R/L)} \frac{1}{q-1}, \quad q \in \mathbb{R}. \quad (2.2)$$

It is derived from the box-counting method, but has better convergence. The idea is that one can randomly choose a point on A , make a sandbox (i.e., a ball with radius R) around it, then count the number of points in A that fall in this sandbox of radius R , represented as $M(R)$ in the above definition. Here, L is the linear size of A . The brackets $\langle \cdot \rangle$ mean to take statistical average over randomly chosen centers of the sandboxes.

The generalized dimension D_q is then obtained by performing a linear regression of the logarithm of sampled data $\ln(\langle [M(R)]^{q-1} \rangle)$ vs. $(q-1)\ln(R/L)$ and taking its slope as the multifractal dimension in a practical use of the sandbox method. The idea can be illustrated by rewriting Eq. (2.2) as

$$\ln(\langle [M(R)]^{q-1} \rangle) = D_q(R/L) \times (q-1) \ln(R/L) + (q-1) \ln(M_0). \quad (2.3)$$

First, we choose R in an appropriate range $[R_{\min}, R_{\max}]$. For each chosen R , we compute the statistical average of $[M(R)]^{q-1}$ over a large number of radius- R sandboxes randomly distributed on A , $\langle [M(R)]^{q-1} \rangle$, then plot the data on the $\ln(\langle [M(R)]^{q-1} \rangle)$ vs. $(q-1)\ln(R/L)$ plane. We next perform a linear regression and calculate the slope as an approximation of the multifractal dimension D_q . The value D_1 is the information dimension and D_2 the correlation dimension of the measure. The D_q values for positive values of q are associated with the regions where the points are dense. The D_q values for negative values of q are associated with the structure and properties of the most rarefied regions.

As an example, we compute and plot the D_q curves for the D_{st} index at different resolutions in Fig. 4. It is clear that these curves exhibit a multifractal-like form at every resolution.

2.3. Recurrent iterated function system for a multifractal measure

In this paper, we model the measure μ of a CGR by a recurrent iterated function system [6,7,16]. This technique has been applied successfully to fractal image compression [5], fractal construction [27] and genomics [1,2,31,32], for exam-

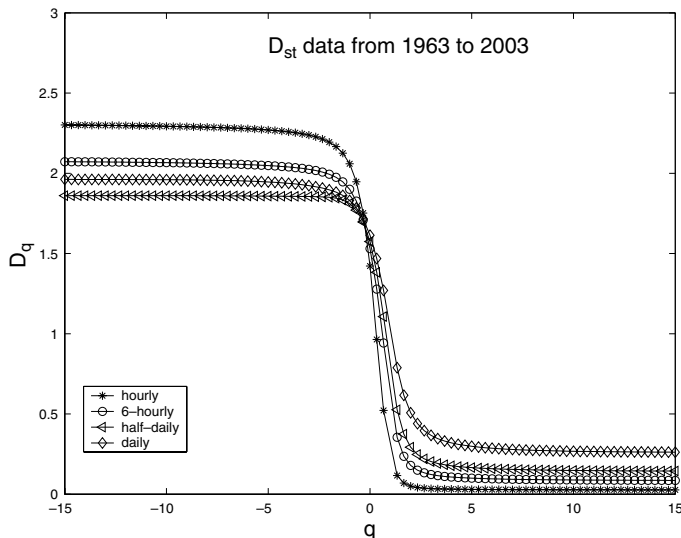


Fig. 4. The D_q curves for the D_{st} index at different resolutions.

ple. Consider a system of contractive maps $S = \{S_1, S_2, \dots, S_N\}$ and the associated matrix of probabilities $\mathbf{P} = (p_{ij})$ such that $\sum_j p_{ij} = 1$, $i = 1, 2, \dots, N$. We consider a random sequence generated by a dynamical system

$$x_{n+1} = S_{\sigma_n}(x_n), \quad n = 0, 1, 2, \dots, \tag{2.4}$$

where x_0 is any starting point and σ_n is chosen among the set $\{1, 2, \dots, N\}$ with a probability that depends on the previous index σ_{n-1} : $P(\sigma_{n+1} = i) = p_{\sigma_n, i}$. Then (S, \mathbf{P}) is called a *recurrent iterated function system*. A major result for RIFS is that there exists a unique invariant measure μ of the random walk (2.4) whose support is the attractor of the RIFS (S, \mathbf{P}) [7].

The coefficients in the contractive maps and the probabilities in the RIFS are the parameters to be estimated for the measure that we want to simulate. We now describe the method of moments to perform this task. In the two-dimensional case of our CGRs, we consider a system of N contractive maps

$$S_i = s_i \begin{pmatrix} x \\ y \end{pmatrix} + \begin{pmatrix} b_1(i) \\ b_2(i) \end{pmatrix}, \quad i = 1, 2, \dots, N.$$

If μ is the invariant measure and A the attractor of the RIFS in \mathbb{R}^2 , the moments of μ are

$$g_{mn} = \int_A x^m y^n d\mu = \sum_{j=1}^N \int_{A_j} x^m y^n d\mu_j = \sum_{j=1}^N g_{mn}^{(j)}.$$

Using the properties of the Markov operator defined by (S, \mathbf{P}) [27], we get

$$g_{mn}^{(i)} = \int_{A_i} x^m y^n d\mu_i = \sum_{j=1}^N p_{ji} \int_{A_j} (s_j x + b_1(j))^m (s_j y + b_2(j))^n d\mu_j = \sum_{j=1}^N p_{ji} \sum_{k=0}^m \sum_{l=0}^n \binom{m}{k} \binom{n}{l} s_j^{k+l} b_1(j)^{m-k} b_2(j)^{n-l} g_{kl}^{(j)}. \tag{2.5}$$

When $n = 0, m = 0$,

$$g_{00}^{(i)} = \sum_{j=1}^N p_{ji} g_{00}^{(j)}, \quad \sum_{j=1}^N g_{00}^{(j)} = 1, \quad \sum_{j=1}^N (p_{ji} - \delta_{ij}) g_{00}^{(j)} = 0. \tag{2.6}$$

When $m = 0, n \geq 1$,

$$g_{0n}^{(i)} = \sum_{j=1}^N p_{ji} \sum_{l=0}^n \binom{n}{l} s_j^l b_2(j)^{n-l} g_{0l}^{(j)},$$

hence the moments are given by the solution of the linear equations

$$\sum_{j=1}^N (s_j^n p_{ji} - \delta_{ij}) g_{0n}^{(i)} = - \sum_{l=0}^{n-1} \binom{n}{l} \sum_{j=1}^N s_j^l b_2(j)^{n-l} p_{ji} g_{0l}^{(j)}, \quad j = 1, \dots, N. \quad (2.7)$$

When $n = 0, m \geq 1$,

$$g_{m0}^{(i)} = \sum_{j=1}^N p_{ji} \sum_{k=0}^m \binom{m}{k} s_j^k b_1(j)^{m-k} g_{k0}^{(j)},$$

hence the moments are given by the solution of the linear equations

$$\sum_{j=1}^N (s_j^m p_{ji} - \delta_{ij}) g_{m0}^{(i)} = - \sum_{k=0}^{m-1} \binom{m}{k} \sum_{j=1}^N s_j^k b_1(j)^{m-k} p_{ji} g_{k0}^{(j)}, \quad j = 1, \dots, N. \quad (2.8)$$

When $m, n \geq 1$,

$$g_{mn}^{(i)} = \sum_{j=1}^N p_{ji} \sum_{k=0}^{m-1} \sum_{l=0}^n \binom{m}{k} \binom{n}{l} s_j^{k+l} b_1(j)^{m-k} b_2(j)^{n-l} g_{kl}^{(j)} + \sum_{l=0}^{n-1} \binom{n}{l} s_j^{m+l} b_2(j)^{n-l} g_{ml}^{(j)} + \sum_{j=1}^N p_{ji} s_j^{m+n} g_{mn}^{(j)},$$

hence the moments are given by the solution of the linear equations

$$\begin{aligned} \sum_{j=1}^N (s_j^{m+n} p_{ji} - \delta_{ij}) g_{mn}^{(i)} = & - \sum_{k=0}^{m-1} \sum_{l=0}^{n-1} \binom{m}{k} \binom{n}{l} \sum_{j=1}^N s_j^{k+l} b_1(j)^{m-k} b_2(j)^{n-l} p_{ji} g_{kl}^{(j)} \\ & - \sum_{l=0}^{n-1} \binom{n}{l} \sum_{j=1}^N s_j^{m+l} b_2(j)^{n-l} p_{ji} g_{ml}^{(j)} - \sum_{k=0}^{m-1} \binom{m}{k} \sum_{j=1}^N s_j^{k+n} b_1(j)^{m-k} p_{ji} g_{kn}^{(j)}, \quad i = 1, \dots, N. \end{aligned} \quad (2.9)$$

If we denote by G_{mn} the moments obtained directly from a given measure, and g_{mn} the formal expression of moments obtained from the above formulae, then solving the optimization problem

$$\min_{s_i, b_1(i), b_2(i), p_{ij}} \sum_{m,n} (g_{mn} - G_{mn})^2$$

will provide the estimates of the parameters of the RIFS.

Once the RIFS $(S_j(x), p_{ji}, i, j = 1, \dots, N)$ has been estimated, its invariant measure can be simulated in the following way: Generate the attractor A of the RIFS via the random walk (2.4). Let χ_B be the indicator function of a subset B of the attractor A . From the ergodic theorem for RIFS [7], the invariant measure is then given by

$$\mu(B) = \lim_{n \rightarrow \infty} \left[\frac{1}{n+1} \sum_{k=0}^n \chi_B(x_k) \right].$$

By definition, an RIFS describes the scale invariance of a measure. Hence a comparison of the given measure with the invariant measure simulated from the RIFS will confirm whether the given measure has this scaling behavior. This comparison can be undertaken by computing the cumulative walk of a measure visualized as intensity values on a $J \times J$ mesh; here $J = 128$ in our examples. The cumulative walk is defined as $F_j = \sum_{i=1}^j (f_i - \bar{f})$, $j = 1, \dots, J \times J$, where f_i is the intensity of the i th point on the extended row formed by concatenating all the rows of the $J \times J$ mesh, and \bar{f} is the average value of all the intensities on the mesh.

Returning to the D_{st} example of Section 2.2 with four levels, an RIFS with four contractive maps $\{S_1, S_2, S_3, S_4\}$ is fitted to the measure representation using the method of moments, and the resulting invariant measure is plotted in Fig. 5. The cumulative walks of these two measures are reported in Fig. 6. It is seen that the fitted RIFS provides an excellent model of the scaling behavior of this D_{st} time series.

3. Prediction of storm events

3.1. Data analysis

The raw data set used in this work comes from the World Data Center (WDC-Kyoto) where an uninterrupted hourly time series is available from 1963 to the present time. We will use the period 1963–2003 in this work. The daily D_{st} time series from 1963 through 2003 is shown in Fig. 1. The time series appears stationary at this scale and a striking

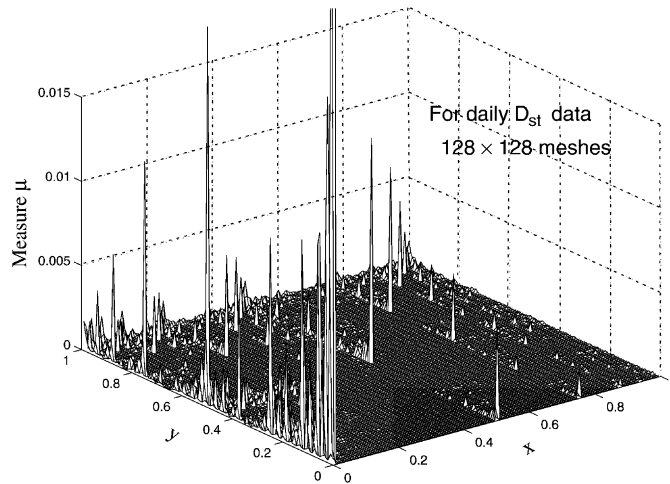


Fig. 5. The RIFS simulation of the measure shown in Fig. 3.

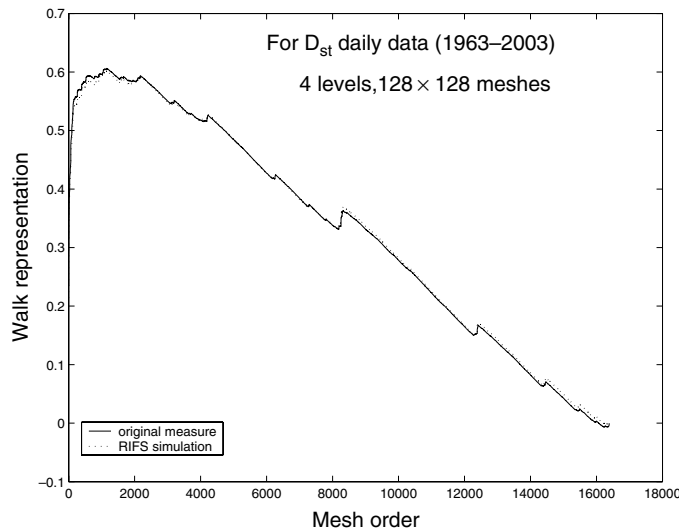


Fig. 6. The walk representation of measures in Figs. 3 and 5.

feature is its bursty negative excursions corresponding to intense storm events. In fact, zooming in on shorter time intervals shows the same pattern. This apparent scaling and intermittency of D_{st} suggests that multifractal techniques would be suitable for its analysis and prediction, which is what we follow in this paper.

In Section 2.1, we considered the D_{st} index with four levels. In the next illustration, we consider 3-symbol scenarios by assuming that the D_{st} index is classified into three categories: $D_{st} \leq -50$; $-50 < D_{st} \leq -30$; $-30 < D_{st}$, which correspond to intense- or moderate-storm, small-storm and no-storm types respectively. We then define the map

$$f_2 = \begin{cases} 0, & \text{if } D_{st} > -30 \text{ nT}, \\ 1, & \text{if } -50 \text{ nT} < D_{st} \leq -30 \text{ nT}, \\ 2, & \text{if } D_{st} \leq -50 \text{ nT}. \end{cases}$$

Under f_2 , the given D_{st} time series is transformed into a symbolic sequence $\{s_i\}$, where s_i is a symbol of the alphabet $\{0, 1, 2\}$. The CGR of this case is given in Fig. 7.

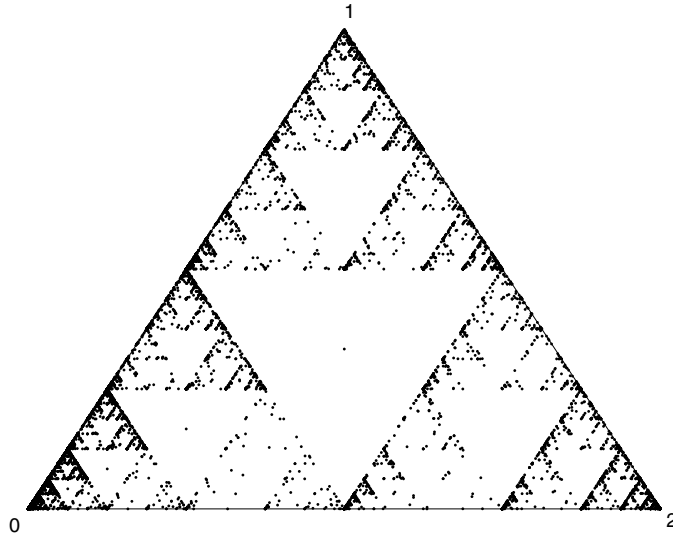


Fig. 7. The three-symbol CGR of daily D_{st} time series from 1963–2003.

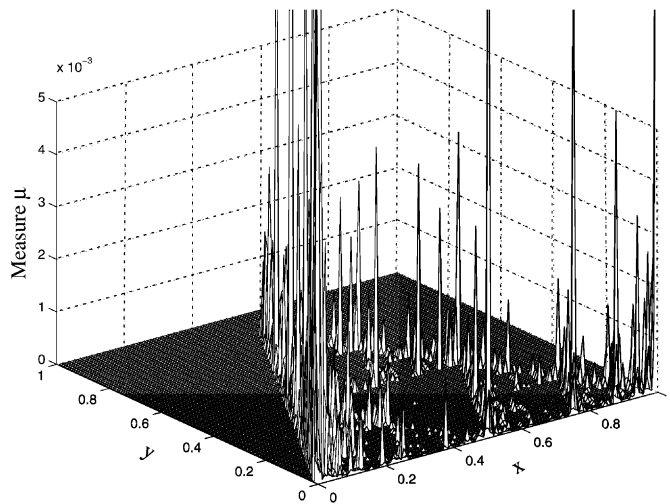


Fig. 8. The measure μ based on a 128×128 mesh of the CGR of Fig. 7.

Considering the points in this CGR, the measure μ defined by $\mu(B) = \#(B)/N_1$ as before is plotted in Fig. 8 on a 128×128 mesh. An RIFS with three contractive maps $\{S_1, S_2, S_3\}$ is fitted to this measure using the method of moments, and the resulting invariant measure is plotted in Fig. 9. The cumulative walks of these two measures are reported in Fig. 10. It is seen that the fitted RIFS provides a good model for the CRG, but the 4-symbol setting of Section 2.1 provides a far superior fit. Hence we will use the 4-symbol model for prediction of future events in the next subsection.

3.2. Prediction

From the available D_{st} time series over 1963–2003, we use the data over the period 1963–1992 for RIFS model fitting and the data over the last 11 years (1993–2003) for testing the accuracy of our prediction. The method therefore provides true outside-sample predictions. We use the map f_1 to convert the time series into a symbolic sequence of the

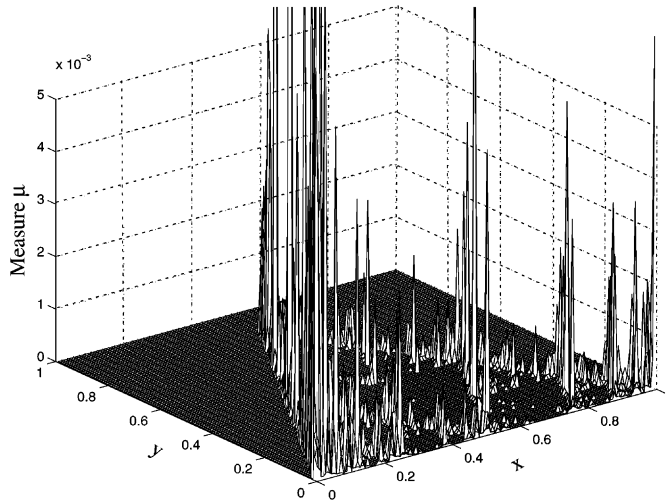


Fig. 9. The RIFS simulation of the measure shown in Fig. 8.

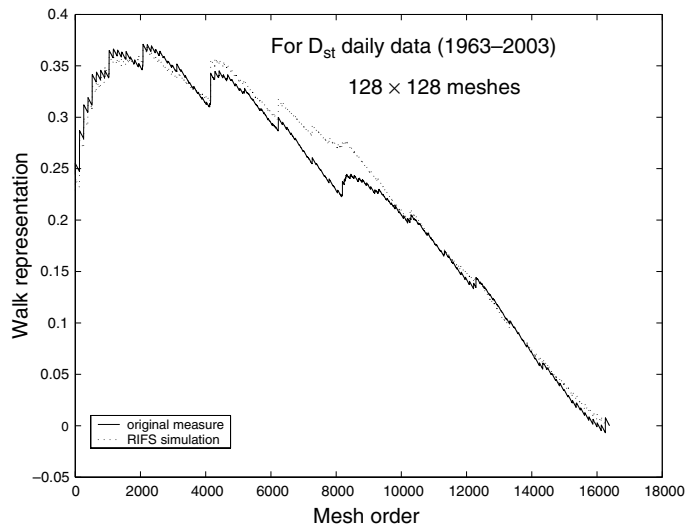


Fig. 10. The walk representation of measures in Figs. 8 and 9.

alphabet $\{0, 1, 2, 3\}$. The fitted RIFS of Section 2.3 is then used to predict future events according to the chaos game algorithm (2.4). That is, knowing the parameters of the stochastic matrix $\mathbf{P} = (p_{ij})$ and the current observation σ_n , a string for $\{\sigma_{n+1}, \dots, \sigma_{n+k}\}$ for k steps ahead on the alphabet $\{0, 1, 2, 3\}$ is generated via (2.4). The prediction is repeated for the next observation σ_{n+1} , using the same estimated model, until the last time point $T - k$ is reached, where T is the number of points of the time series.

We then compare with real events as known from the data, and determine the accuracy of the prediction according to the following two indicators:

$$r_1 = \frac{\text{number of correct predictions}}{\text{total number of predictions}};$$

$$r_2 = \frac{\text{number of storm events predicted to contain a storm event}}{\text{number of real strings containing a storm event}}.$$

Table 1
Prediction of daily data using map f_1

Days ahead	r_1	r_2
1	2180/3675 = 59.32%	925/1444 = 64.06%
2	1388/3674 = 37.78%	1127/1846 = 61.05%
3	940/3673 = 25.59%	1183/2154 = 64.21%
4	624/3672 = 16.99%	1652/2417 = 68.35%

In r_2 , the predicted pattern of k -days ahead is not required to be the same as the observed pattern. The results are reported in Table 1.

4. Conclusion

Based on the values recorded, the D_{st} is clustered into events such as {intense storm, moderate-storm, small-storm, no-storm}. Some previous works have suggested the values to distinguish these events; for example, storms with $D_{st} < -50$ nT are classified as moderate or intense, and those in the range -50 nT $\leq D_{st} < -30$ nT classified as small storms [18,30]. In this way, the D_{st} time series is converted into a sequence of symbols {0, 1, 2, 3} accordingly. A chaos game representation and its probability measure are then derived for the symbolic sequence.

The work of this paper indicates that each of these probability measures is a multifractal measure and can be modeled by a set of contractive maps known as a recurrent iterated function system. The excellent fit of this RIFS to data confirms that the attractor/fractal set of the RIFS is in fact the CRG of the symbolic sequence. The fitted RIFS is considered as a mechanism to generate the weighting of storm events. This mechanism is the key element in our algorithm for prediction of storm events described in Section 3.2.

In this paper, we pay attention to the prediction of storm events in the next few days using daily data. The numerical results summarised in the above table indicate that the method works reasonably well on real data up to four days ahead based on the indicator r_2 . It should be noted that these are outside-sample forecasts of true storm events based on only the current value at σ_n ; hence it is expected that the prediction is more difficult than those methods designed for the prediction of the frequency/probability of storm patterns. An accuracy rate of over 60% in r_2 is therefore quite meaningful. A further point to note is that this accuracy is achieved from the scaling of the D_{st} series captured in its chaos game representation. This distinguishes our approach from the usual approach based on the correlation structure of D_{st} . This latter approach would not be suitable for the D_{st} time series where intermittency and non-Gaussianity are dominant features.

Acknowledgement

This work is partially supported by the NSF grant DMS-0417676, the ARC grant DP0559807 and the NSFC grant 30570426. The authors would like to thank Prof. M.S. El Naschie, the editor-in-chief of this journal to point out more applications of chaos game technique.

References

- [1] Anh VV, Lau KS, Yu ZG. Multifractal characterisation of complete genomes. *J Phys A Math Gen* 2001;34:7127.
- [2] Anh VV, Lau KS, Yu ZG. Recognition of an organism from fragments of its complete genome. *Phys Rev E* 2002;66:031910.
- [3] Anh VV, Yu ZG, Wanliss JA, Watson SM. Prediction of magnetic storm events using the D_{st} index. *Nonlinear Process Geophys* 2005;12:799–806.
- [4] Ayache A, Lévy Véhel J. The generalized multifractional Brownian motion. *Statist Inference Stochast Process* 2000;3:7–18.
- [5] Barnsley MF. *Fractals everywhere*. New York: Academic Press; 1988.
- [6] Barnsley MF, Demko S. Iterated function systems and the global construction of fractals. *Proc R Soc London Ser A* 1985;399:243.
- [7] Barnley MF, Elton JH, Hardin DP. Recurrent iterated function systems. *Constr Approx B* 1989;5:3–31.
- [8] Burlaga LF. Multifractal structure of the interplanetary magnetic field: Voyager 2 observations near 25 AU, 1987–1988. *Geophys Res Lett* 1991;18(1):69.
- [9] Burlaga LF. Lognormal and multifractal distributions of the heliospheric magnetic field. *J Geophys Res* 2001;106:15917.

- [10] Burlaga LF, Wang C, Ness NF. A model and observations of the multifractal spectrum of the heliospheric magnetic field strength fluctuations near 40 AU. *Geophys Res Lett* 2003;30. doi:10.1029/2003GL016903.
- [11] Burton RK, McPherron RL, Russell CT. An empirical relationship between interplanetary conditions and Dst. *J Geophys Res* 1975;80:4204.
- [12] El Naschie MS. double-slit experiment, Heisenberg uncertainty principle and Cantorian space-time. *Chaos Solitons and Fractals* 1994;4(3):403–9.
- [13] El Naschie MS. Quantum measurement, diffusion and Cantorian geodesics. *Chaos, Solitons & Fractals* 1994;4(7):1235–47.
- [14] El Naschie MS. Iterated function systems and the two-slit experiment of quantum mechanics. *Chaos, Solitons & Fractals* 1994;4(10):1965–8.
- [15] El Naschie MS. Iterated function in systems, information and the two-slit experiment of quantum mechanics. In: El Naschie MS, Rössler OE, Prigogine I, editors. *Quantum mechanics, diffusion and chaotic fractals*. Oxford: Pergamon-Elsevier; 1995. p. 185–8.
- [16] Falconer K. *Techniques in fractal geometry*. Wiley; 1997.
- [17] Fiser A, Tusnady GE, Simon I. Chaos game representation of protein structures. *J Mol Graphics* 1994;12:302–4.
- [18] Gonzalez WD, Joselyn JA, Kamide Y, Kroehl HW, Rostoker G, Tsurutani BT, et al. What is a geomagnetic storm? *J Geophys Res* 1994;99:5771.
- [19] Greenspan ME, Hamilton DC. A test of the Dessler–Parker–Sckopke relation during magnetic storms. *J Geophys Res* 2000;105:5419.
- [20] Halsey T, Jensen M, Kadanoff L, Procaccia I, Schraiman B. Fractal measures and their singularities: the characterization of strange set. *Phys Rev A* 1986;33:1141–51.
- [21] Jeffrey HJ. Chaos game representation of gene structure. *Nucl Acids Res* 1990;18:2163–70.
- [22] Kabin K, Papitashvili VO. Fractal properties of the IMF and the Earth's magnetotail field. *Earth Planets Space* 1998;50:87.
- [23] Lui ATY, Chapman SC, Liou K, Newell PT, Meng CI, Brittnacher M, et al. Is the dynamic magnetosphere an avalanching system? *Geophys Res Lett* 2000;27:911.
- [24] Lui ATY. Multiscale phenomena in the near-Earth magnetosphere. *J Atmos Sol-Terr Phys* 2002;64:125.
- [25] Lui ATY, Lai WW, Liou K, Meng CI. A new technique for short-term forecast of auroral activity. *Geophys Res Lett* 2003;30:1258.
- [26] Tél T, Flülöp A, Vicsek T. Determination of fractal dimensions for geometrical multifractals. *Physica A* 1989;159:155–66.
- [27] Vrscay ER. In: *Fractal geometry and analysis*. In: Belair J, Dubuc S, editors. NATO Advanced Study Institute, Series C: Mathematical and physics sciences, vol. 346. Dordrecht, The Netherlands: Kluwer Academic; 1991.
- [28] Wanliss JA. Nonlinear variability of SYM-H over two solar cycles. *Earth Planets Space* 2004;56:e13–6.
- [29] Wanliss JA. Fractal properties of SYM-H during quiet and active times. *J Geophys Res* 2005;110:A03202.
- [30] Wanliss JA, Anh VV, Yu ZG, Watson S. Multifractal modelling of magnetic storms via symbolic dynamics analysis. *J Geophys Res* 2005;110:A08214.
- [31] Yu ZG, Anh VV, Lau KS. Measure representation and multifractal analysis of complete genomes. *Phys Rev E* 2001;64:031903.
- [32] Yu ZG, Anh VV, Lau KS. Iterated function system and multifractal analysis of biological sequences. *Int J Mod Phys B* 2003;17:4367–75.
- [33] Yu ZG, Anh VV, Lau KS. Chaos game representation of protein sequences based on the detailed HP model and their multifractal and correlation analyses. *J Theor Biol* 2004;226:341–8.